Direct Measurement of an Electron Bernstein Wave on the Internal Coil Device Mini-RT

E. Yatsuka, D. Sakata, K. Kinjo, J. Morikawa[a)], Y. Ogawa[a)]

Graduate School of Frontier Sciences, Univ. Tokyo, 5-1-5 Kashiwa-no-ha, Kashiwa-shi, Chiba 277-8561, Japan

[a)]High Temperature Plasma Center, Univ. Tokyo, 5-1-5 Kashiwa-no-ha, Kashiwa-shi, Chiba 277-8568, Japan

(Received 15 October 2007)

Measurements of electron cyclotron range of frequencies (ECRF) electric fields by using small (5 mm) antenna have been carried out in the Mini-RT device, and signals having two characteristics of electron Bernstein wave (EBW) have been detected. One of them is short wavelength (~2 cm). The order of corresponding refractive index is 10, while calculation predicts several 10 to 100. The other characteristic is backward wave, i.e. group velocity is opposite to phase velocity. In the Mini-RT device, plasma production is achieved by using ECH, therefore we can expect the existence of high-energy electrons. High-energy electrons can affect dispersion relation, and waves having relatively long wavelength can propagate around upper hybrid resonance (UHR).

Keywords: electron Bernstein wave, mode conversion, electrostatic mode, backward wave, overdense plasma, density gradient, cyclotron harmonic resonance, upper hybrid resonance, interferometry, antenna

Electron Bernstein Wave (EBW) is one of the most promising methods for high beta plasma heating. This wave can propagate across magnetic surfaces without density limit and strongly be damped due to cyclotron harmonic damping. However, EBW is an electrostatic mode and its wavelength is comparable to electron Lamor radius [1], thus it is hard to launch EBW directly into plasma except for the special case as slender plasma, e.g. glow discharge positive column plasma [2]. In Ref. [2], the first observation of EBW radiation, i.e. inverse process of absorption, was discussed.

Excitation of EBW in plasma via mode conversion process [3] is needed to achieve EBW heating for thick plasma, e.g. fusion plasma. In linear device, electron cyclotron range of frequency (ECRF) electric field in plasma was investigated by using wire antenna [4]. As a result, mode-converted EBW was observed with so-called fast X-B method. Recently, mode conversion efficiencies have been evaluated by using electron cyclotron emission (ECE) via mode conversion from EBW to electromagnetic waves [5,6]. This method is suitable for studying EBW heating without disturbance, but it is hardly applicable for devices that have steep magnetic field gradient such as internal coil device.

Internal coil devices have been constructed to investigate high beta plasma confinement [7,8], which is based on the theory of self-organized states in flowing plasma [9]. The objective of this research is production of highly overdense plasma by using EBW heating.

author's e-mail: yatsuka@ppl.k.u-tokyo.ac.jp

This Letter reports the preliminary results of ECRF electric field measurements in the internal coil device Mini-RT (Miniature Ring Trap). We produce plasma by injecting an X-mode microwave (2.45 GHz, 2.5 kW c.w.). High Temperature Superconductiong (HTS) Coil, that is called Floating Coil (F-Coil), produces poloidal magnetic field, which is similar to that of a planet. Typical strength of magnetic field is 0.01-0.1 T. Figure 1 shows two magnetic configurations in Mini-RT, i.e. (a) Dipole configuration and (b) Separatrix configuration. Solid (Dotted) lines denote magnetic surfaces (magnetic field strengths). Figure 2 shows typical radial profiles of electron density; (i) Dipole configuration, (ii) Separatrix configuration. By applying Levitation Coil (L-Coil)

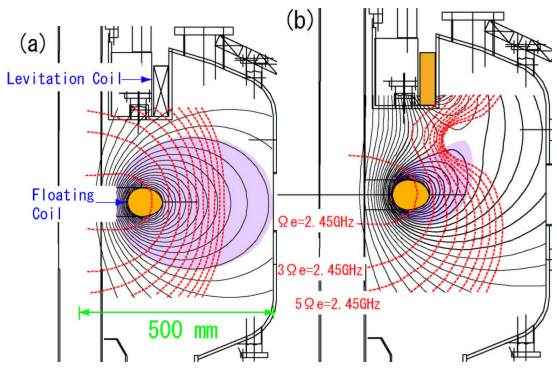

Fig.1 Cross section of the Mini-RT device. (a) Dipole configuration (L-Coil current is not applied) (b) Separatrix configuration

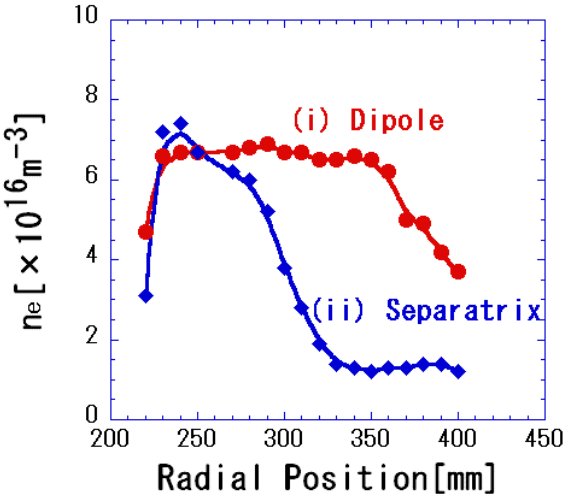

Fig.2 Radial profiles of electron density n_e. (i) Dipole configuration, (ii) Separatrix configuration.

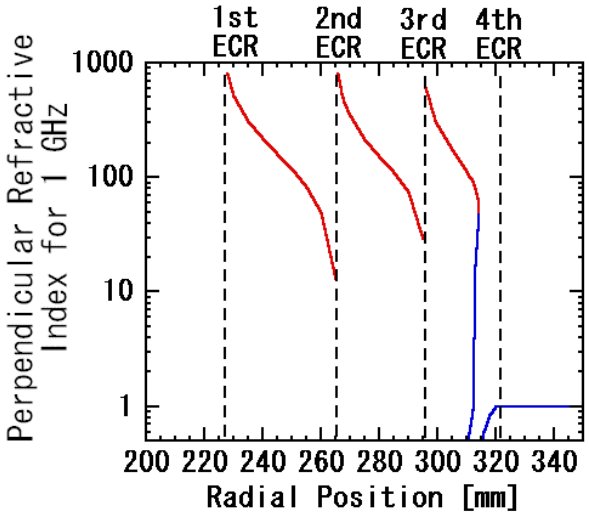

Fig.3 Perpendicular refractive index of hot wave with typical density profile of Mini-RT.

current, we can produce separatrix, and plasma is confined in closed flux surfaces. We can also create steep density gradient region (L_n ~ 5 cm) around separatrix [10,11]. Peak density is around cut-off density of 2.45GHz, O-Mode microwave, i.e. 7.6×10^{16} m^{-3}.

Dispersion relation predicts that typical value of perpendicular refractive index of EBW is several 10 to 100. Figure 3 shows calculated radial profile of refractive index on mid-plane for 1.0 GHz. We assumed trapezoidal density profile, which is similar to Fig. 2 (ii); and electron temperature is uniformly 10 eV, which is typical value of Langmuir probe measurements [11]. We calculated dispersion relation of hot wave [12] propagating

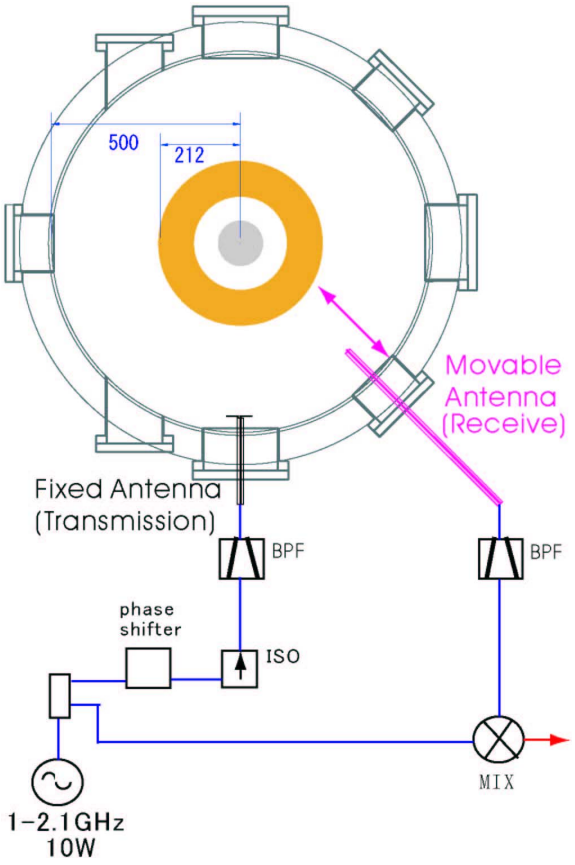

Fig.4 Top view of Mini-RT and block diagram of circuit.

perpendicular to magnetic field. We assumed perpendicular injection of X-Mode from low field side, which is one of the most appropriate for mode conversion to EBW. Injected X-Mode electromagnetic wave tunnels evanescent region which lies between right hand cut-off (R-Cutoff) and upper hybrid resonance (UHR), i.e. 310 < R < 315 mm. Energy of X-wave transfers into EBW around UHR.

Mode conversion efficiency C have been evaluated by

$$C = 4e^{-\pi\eta}(1-e^{-\pi\eta})\cos^2(\phi/2+\theta), \qquad (1a)$$

$$\eta = \frac{\Omega_e L_n}{c}\frac{\alpha}{\sqrt{\alpha^2+2L_n/L_B}}\left[\frac{\sqrt{1+\alpha^2}-1}{\alpha^2+(L_n/L_B)\sqrt{1+\alpha^2}}\right]^{1/2}, \qquad (1b)$$

$$\alpha = \left.\frac{\omega_{pe}}{\Omega_e}\right|_{UHR}, \qquad (1c)$$

where c, Ω_e, ω_{pe}, L_n and L_B are light speed, electron cyclotron frequency, electron plasma frequency,

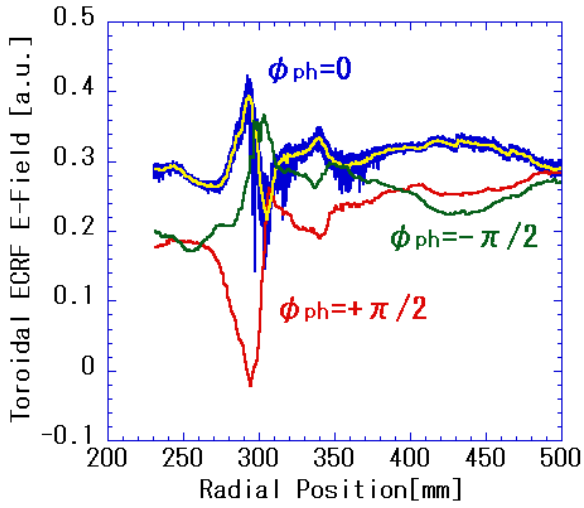

Fig.5 Interferometer traces for $\phi_{ph} = \pm\pi/2$, 0. Frequency of a launched wave was 1.0 GHz. We can obtain fluctuated data, and signals are averaged over each millimeter to determine amplitude and phase of an ECRF electric field.

characteristic length of density and that of magnetic field, respectively [13,14]; and ϕ is the phase difference between X-Mode propagating toward L-Cutoff and reflected component propagating toward the UHR; and θ is the phase of $\Gamma(i\eta/2)$. By using expression (1a) without considering phase effect, i.e. term of cosine is unity, we obtain 70~90 % mode conversion efficiency with separatrix configuration in Mini-RT.

To investigate mode conversion process in plasma directly, we launch X-Mode microwave by using ceramic-coated dipole antenna (element length is 100 mm). Frequency and power of diagnostic microwave are 1-2.1 GHz, 10 W, respectively. By using lower frequencies than plasma heating, i.e. 2.45 GHz, we can investigate waves in overdense plasma even where underdense region of heating microwave. To avoid penetration of high power of microwave with 2.45GHz, we set band pass filter (BPF, -44.5 dB @2.45 GHz). Figure 4 shows the block diagram of ECRF electric field measurements. We can obtain DC voltage signal

$$E_0(\vec{r}) + E_1(\vec{r})\cos[\phi(\vec{r}) + \phi_{ph}], \qquad (2)$$

where $E_0(\vec{r})$, $E_1(\vec{r})$, $\phi(\vec{r})$ represent offset, amplitude of ECRF electric field and phase of that, respectively. We can control an external phase shift ϕ_{ph} to determine the parameters $E_0(\vec{r})$, $E_1(\vec{r})$ and $\phi(\vec{r})$. Spatial profiles of ECRF electric fields are detected by using coax-fed monopole (element length is 5mm, direction is toroidal) antenna movable radially.

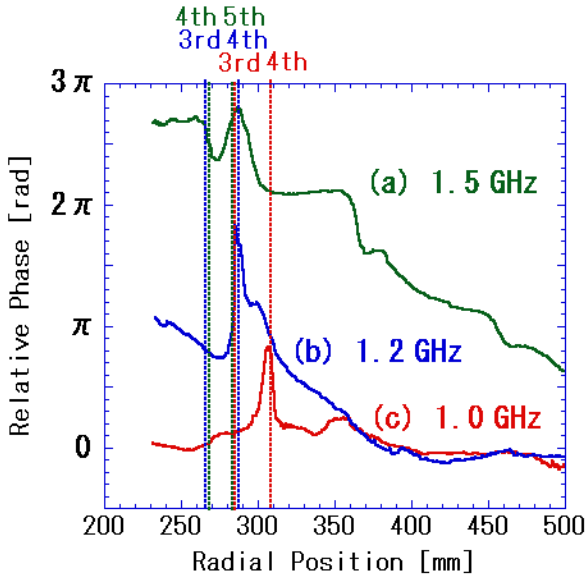

Fig.6 Radial profiles of phase of ECRF electric field with (a) 1.0 GHz, (b) 1.2 GHz, (c) 1.5GHz

Figure 5 shows toroidal component of an ECRF electric field on the mid-plane with separatrix configuration. We can see a characteristic of short wavelength related with the EBW around major radius *R*=300 mm in Fig. 5. Roughly evaluated wavelength of that is 2 cm, while 30cm in vacuum. Therefore the order of refractive index of EBW is 10. Location of the Last Closed Field Surface (LCFS) was major radius *R*~300mm. The EBW was detected at steep density gradient region.

Radial profiles of phase of ECRF electric field with several frequencies are shown in Fig. 6. We used data for three external phase shifts that were averaged over each millimeter. The characteristic of phase reversal has been seen for each frequency. Dotted lines in Fig. 6 denote the location of cyclotron harmonic resonance layers on mid-plane. Phase reversal phenomena occur between 3rd and 4th harmonic ECR for 1.0 and 1.2 GHz, 4th and 5th harmonic ECR for 1.5 GHz. And the location of it coincides with short wavelength region.

We can consider the direction of group velocity, i.e. energy flux, is inward of the device. While positive (negative) gradient of relative phase with respect to major radius means phase velocity is outward (inward) of the device. Thus phase reversal region suggests the direction of phase velocity v_{ph} is opposite to group velocity v_g. From the dispersion relation, we can find that the EBW has the characteristic of backward wave, i.e. group velocity v_g is negative [15]. Therefore Fig. 6 also suggests the direct detection of EBWs between cyclotron harmonic resonance surfaces, e.g. 3rd and 4th ECR for 1.0 GHz injection.

As well known, ECH enables to produce high- energy

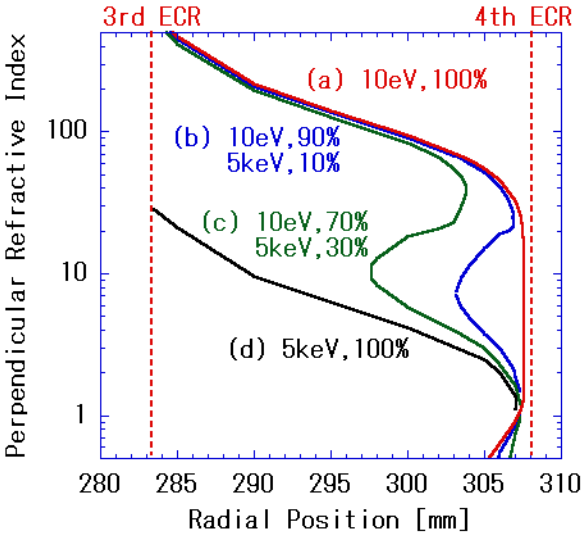

Fig.7 Radial profile of perpendicular refractive indices, for 1 GHz, of hot waves with (a) all electrons has temperature of 10 eV, (b ,c ,d) 10%, 30%, 100% high-energy electrons has that of 5 keV. Dotted lines denote the location of harmonic ECR on mid-plane.

electrons due to quasi-linear diffusion of resonant electrons [16]. In the Mini-RT device, plasma is produced by ECH, thus we have prospects of production of high-energy electrons. We estimate effective temperature of high-energy electron is 5 keV by using scaling law of Ref. [17].

$$\rho / L = 5 - 6 \times 10^{-2}, \tag{3}$$

where ρ and L are high-energy electron Lamor radius and magnetic scale length, respectively. We have estimated $L \sim 4$ cm and $B = 0.0875$ T.

We have assumed electron distribution function is two components isotropic Maxwellian, i.e. summation of bulk electrons (10 eV) and high-energy electrons (5 keV), for simplicity. We have calculated for four cases, i.e. (a) no high-energy electrons, (b) 10% of them exist, (c) 30% of them exist and (d) hot electrons. We have also assumed F-Coil current I_F is 30 kA and L-Coil current I_L is 15 kA, which are equal conditions for Figs. 5 and 6. In this configuration, mode conversion occurs between 3rd and 4th harmonics of ECR. Dispersion relation of hot waves propagating perpendicular to magnetic field is written as

$$\varepsilon_{xx}(\varepsilon_{yy} - n^2) - \varepsilon_{xy}\varepsilon_{yx} = 0, \tag{4}$$

where n and ε are refractive index and specific dielectric tensor of hot waves [12], respectively.

High-energy electrons affect dispersion relation of hot wave especially around the UHR. If there is no high-energy electron, i.e. in the case of (a), refractive index dramatically rises around UHR. Refractive indices have relatively long wavelength region (refractive index is small) with increasing of high-energy electrons. The reason why refractive indices, for (b) and (c), are so complex is due to assumption of two components Maxwellian distribution function. Finite Lamor radius (FLR) effect from high-energy electrons around UHR enables propagation with long wavelength.

On the other hand, refractive indices show identical characteristics around 3rd harmonic ECR, for the case with (a), (b) and (c) of Fig. 7. Around resonance region, wavelength is comparable to Lamor radius, therefore sufficient FLR effect from bulk electrons can be expected.

In summary, ECRF electric field measurements by using antenna have been carried out in the Mini-RT device. And signals having two characteristics of EBW, i.e. short wavelength (~ 2 cm) and backward wave, have been detected. Dispersion relation predicts that typical value of refractive index of EBW in Mini-RT is several 10 to 100. However roughly evaluated refractive index is 10 experimentally. Plasma production in Mini-RT is achieved by ECH, therefore we can expect the existence of high-energy electrons. We evaluated the effects of high-energy electrons to dispersion relation, and obtained relatively long wavelength region around UHR.

The authors would like to acknowledge Dr. T. Kaneko for his technical advices for measurements. The authors also thank to Prof. T. Mito and Dr. N. Yanagi for discussion about cooling superconducting magnet and excitation of it.

[1] I. B. Bernstein, Phys. Rev. **109**, 10 (1958).
[2] K. Mitani and H. Kubo, J. Phys. Soc. Jpn. **19**, 211 (1964).
[3] T. H. Stix, Phys. Rev. Lett. **23**, 878 (1965).
[4] H. Sugai, Phys. Rev. Lett. **47**, 1899 (1981).
[5] G. Taylor *et al*., Phys. Plasmas **9**, 167 (2002).
[6] B. Jones *et al*., Phys. Rev. Lett. **90**, 165001 (2003).
[7] Y. Ogawa *et al*., J. Plasma Fusion Res. **79**, 643 (2003).
[8] Z. Yoshida *et al*., Plasma Fusion Res. **1**, 008 (2006).
[9] S. M. Mahajan and Z. Yoshida, Phys. Rev. Lett. **81**, 4863 (1998).
[10] T. Goto *et al*., Jpn. J. Apl. Phys. **45**, 5197 (2006).
[11] E. Yatsuka *et al*., Trans. Fusion Sci. Tech. **51**, 310 (2007).
[12] T. H. Stix, *Waves in Plasmas* (American Institute of Physics, 1992) p. 257-262.
[13] A. K. Ram and S. D. Schultz, Phys. Plasmas **7**, 4084 (2000).
[14] A. K. Ram *et al*., Phys. Plasmas **3**, 1976 (1996).
[15] F. W. Crawford *et al*., J. Geophys. Res. **72**, 57 (1967).
[16] C. F. Kennel and F. Engelmann, Phys. Fluids **9**, 2377 (1966).
[17] N. A. Uckan, Phys. Fluids **25**, 2381 (1982).